557

T-stress solutions for cracks in rectangular plates with multiple holes

Jackie Yu, Xin Wang[†] and Choon-Lai Tan

*Department of Mechanical and Aerospace Engineering, Carleton University
Ottawa, Ontario, K1S 5B6, Canada*

Abstract. The elastic T-stress is increasingly being recognized as an important second parameter to the stress intensity factor for fracture and fatigue assessments. In this paper, the mutual or M-contour integral approach is employed in conjunction with the Boundary Element Method (BEM) to determine the numerical T-stress solutions for cracks in plates with multiple holes. The problems investigated include plates of infinite width with multiple holes at which single or double, symmetric cracks have grown from. Comparisons of these results are also made with the corresponding solutions of finite plates with a single hole. For completeness, stress intensity factor solutions for the cracked geometries analyzed are presented as well. These results will be useful for failure assessments using the two-parameter linear elastic fracture mechanics approach.

Keywords: T-stress; crack-tip constraint; BEM; plate with multiple holes; M-contour integral.

1. Introduction

Incorporating the elastic T-stress, the leading non-singular term in the Williams' (1957) series expansion, together with the stress intensity factor (SIF), has been shown to provide a more complete assessment of the stress field in the vicinity of a crack, e.g. Larsson and Carlsson (1973), Rice (1974), Bilby *et al.* (1986) and Du and Hancock (1991). It is now well established that the sign and magnitude of the T-stress have implications on the crack-tip stress constraint, and hence the plastic zone size there, as well as crack growth stability and its trajectory. More specifically, positive T-stress leads to higher crack-tip constraint resulting in smaller crack-tip plastic zone size, and vice versa. Indeed, the works of, e.g., Du and Hancock (1991) and Betegon and Hancock (1991), have shown the significance of the T-stress as the second parameter to the J-integral in the characterization of the elastic-plastic crack-tip stress fields for a number of cracked geometries. There is evidence as well that the T-stress can significantly affect the predicted rate of propagation of fatigue cracks, Tong (2002). Roychowdhury and Dodds (2004) have also shown that this parameter can affect the predicted extent of crack closure under cyclic loading. In recognition of its significance, the elastic T-stress has now been incorporated into fracture assessment procedures in design codes, Ainsworth *et al.* (2000, 2002). T-stress solutions for practical geometries and loading conditions are thus useful when applying this two-parameter fracture mechanics methodology.

---

† Associate PROFESSOR, Ph.D., Corresponding author, E-mail: xwang@mae.carleton.ca

Stress concentrations are commonly found in engineering components, and for cracks emanating from them, SIF solutions for numerous geometries and loading conditions are readily available, see e.g. Murakami (2003), Rooke and Cartwright (1976). However, *T*-stress solutions for such problems remain scarce. Wang *et al.* (2006) have recently obtained the *T*-stress for small cracks in notches and holes. Broberg (2004) has obtained *T*-stress solutions for an infinite plate with double-cracks emanating from the edge of a single circular hole under uniform remote tension. *T*-stress solutions for crack(s) emanating from a circular hole in a finite plate under remote tension and bending loads have recently been obtained by Yu *et al.* (2006). In all of the above-mentioned references, there is only one stress concentration in each of the geometries considered. In many practical applications, geometric discontinuities are often in close vicinity of each other, such as the case of rivet holes in aerospace structures. The aim of this paper is to obtain numerical *T*-stress solutions for cracks in plates with multiple circular holes from the edges of which these cracks have grown. Comparisons of these results will be made with the corresponding ones for the case when there is only one circular hole.

2. The boundary element method for *T*-stress determination

The Boundary Element Method (BEM) with the quadratic, isoparametric formulation was employed for the numerical stress analysis in this study. It involves the transformation of the governing differential equations into an integral equation over the boundary. Thus, only the boundary of the solution domain needs to be modelled. This feature offers significant advantages over other numerical schemes, such as the finite element method (FEM), requiring less effort for mesh designs, data preparation, and the computational analysis. BEM is also now widely recognized as a very efficient numerical tool for linear elastic fracture analysis and several associated schemes have now been commonly adopted for stress intensity factor calculations, see, e.g., Aliabadi and Rooke (1986). For the evaluation of the elastic *T*-stress, Sladek *et al.* (1997), has developed a mutual- or *M*-contour integral approach which is more suited for BEM implementation. It is based on the Betti-Rayleigh's reciprocal work theorem and an auxiliary field. Because the contour integral is along a closed path sufficiently far from the crack-tip, it obviates the need to compute the stress field near the vicinity of the crack, where large numerical errors can occur due to the crack-tip stress singularity.

Consider the cracked elastic, isotropic domain R with boundary S, as shown in Fig. 1. Inside this domain, consider a closed integration path comprised of Γ_o, Γ_C^+, and Γ_C^-. A small circular region bounded by Γ_ε near the crack-tip has to be excluded because of the stress singularity there; this region is small and will reduce to zero in a limiting process. The contour of integration $\Gamma = \Gamma_o + \Gamma_C^+ + \Gamma_C^- - \Gamma_\varepsilon$ is a closed path in the counter-clockwise direction. Using Gauss' divergence theorem, Hooke's law and strain-displacement relations, the Betti-Rayleigh's reciprocal theorem for two sets of equilibrium states of the sub-domain can be expressed as

$$\int_\Gamma (t_i u_i' - t_i' u_i) \cdot d\Gamma = \int_\Omega (X_i' u_i - X_i u_i') \cdot d\Omega \tag{1}$$

where u_i are the displacements, t_i are the tractions and X_i are the body forces. The primed and unprimed states correspond to an auxiliary and the unknown fields, respectively. Sladek *et al.* (1997) proposed an auxiliary field which also corresponds to that due to a static point force f
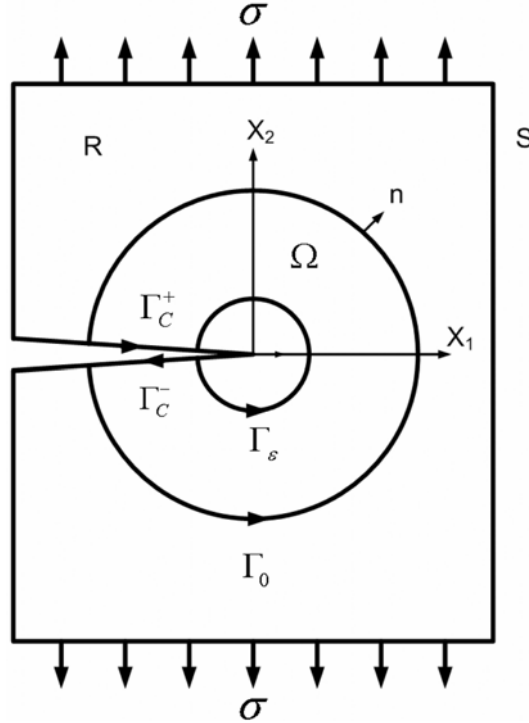
Fig. 1 Contour path around the crack-tip

applied at the crack-tip in the direction parallel to the plane of the crack, as used by Kfouri (1986) in his FEM analysis. However the one adopted by Sladek *et al.* (1997) has one order higher singularity, as it is obtained by differentiating the auxiliary field presented by Kfouri (1986). Following the usual limiting process, an expression relating the *T*-stress to the *M*-integral can be obtained (see Sladek *et al.* (1997)) to be as follows

$$
T = \frac{E}{f(1-v^2)} \int_{\Gamma_0} (t_i' u_i - t_i u_i') \cdot d\Gamma
$$

$$
= \frac{E}{f(1-v^2)} \int_{\Gamma_0} \frac{f}{\pi r^2} \left(F_{ij}(\theta) u_i - t_i \frac{F_{ij}(\theta)}{E} \right) \cdot d\Gamma
$$

(2)

where *E* and *v* are the Young's modulus and Poisson's ratio, respectively, and $F_{ij}(\theta)$ contains known trigonometric functions of the angular location at distance *r* from the crack-tip along the integration path. The corresponding nodal displacements and tractions, u_i and t_i, can be computed from the BEM analysis. Using this approach, Li *et al.* (2004) has obtained *T*-stress solutions for pressurized thick-walled cylinders using BEM while the present authors have also determined similar results for cracks emanating from single circular holes in finite plates. Following similar schemes, Shah *et al.* (2005), in their BEM analysis, have also derived the expression for the *T*-stress in terms of the *M*-contour integral in anisotropic elasticity in two-dimensions.

Although it has been employed (Yu *et al.* 2006, Li *et al.* 2004) to solve for *T*-stress solutions, a test problem is nevertheless presented here to demonstrate the veracity of the BEM analysis.
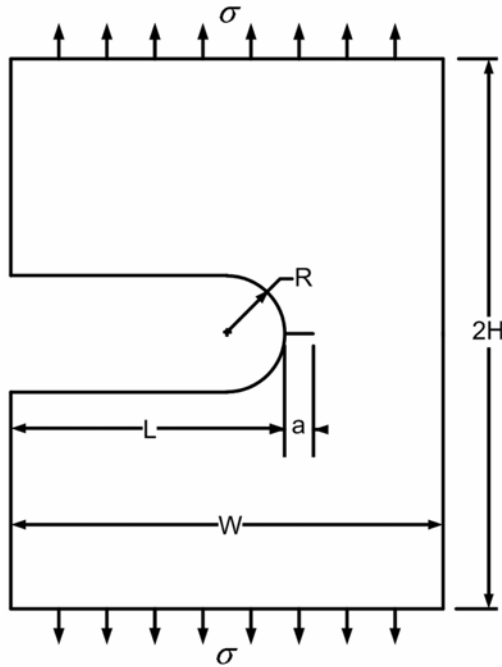
Fig. 2 A finite plate with a crack emanating from a
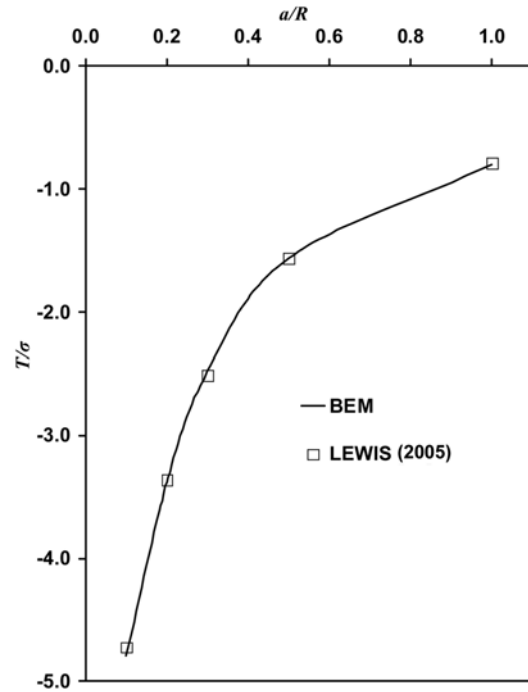U-notch under uniform remote tension

Fig. 3 Comparison of *T*-stress solutions obtained by
Lewis (2005) and those obtained by BEM

Consider the cracked plate with a U-notch as shown in Fig. 2. Using FEM, Lewis (2005) has obtained numerical *T*-stress results for a range of ratios of the geometric parameters for the problem. For the present purpose, only one set of geometry is considered, namely, $L/W = 0.3$, $H/W = 3.0$, $R/W = 0.025$, and relative crack lengths $a/R = 0.1 - 1.0$. Fig. 3 shows the results obtained from the two different numerical approaches, where it can be seen that there is excellent agreement.

3. Numerical analysis

Three different cases of finite height plates with cracks emanating from circular holes are analyzed in this paper. Two of them involve plates of finite height but with an infinite array of holes from which cracks have grown; the centres of these holes are all in the same horizontal plane of the cracks. The third case deals with the influence of two adjacent holes on the *T*-stress of cracks which have developed from a circular hole in an infinitely wide plate; the centres of these holes in this case are aligned in the same vertical plane perpendicular to the cracks. Only remote uniform tension loading by stress σ is considered here throughout. For completeness, the stress intensity factors for these cracks are also determined and presented. Where possible, comparisons with the numerical results for the corresponding cases of those cracks occurring in finite plates with single circular holes will be made.

3.1 Case A – A plate with an infinite array of circular holes, each with a pair of symmetric double cracks at its edge

Fig. 4 shows the physical problem for this case in which R is the radius of the circular holes, a is the effective crack length, $2H$ is the height of the plate and $2W$ is the distance between the centres of the holes. Two values of R/W ratio are considered, namely, $R/W = 0.25$ and $R/W = 0.50$, but the height-to-hole spacing ratio H/W is fixed at 2. The range of the relative crack lengths are $a/R = 1.1 - 3.2$ when $R/W = 0.25$ and $a/R = 1.1 - 1.6$ when $R/W = 0.50$. By virtue of periodic symmetry, only a sector of the problem, as shown in Fig. 5 was modelled in the BEM analysis.

Figs. 6 and 7 show the BEM computed results of the normalized stress intensity factor, $K_I/\sigma\sqrt{\pi(a-R)}$, and the normalized T-stress, T/σ, respectively. Also shown in the figures are the corresponding solutions for the case of a finite plate (width $2W$, height $2H$; $H/W = 2$) with a central circular hole as obtained by Yu *et al.* (2006). Although the trends are similar, it can be seen that the normalized stress intensity factor for the same relative crack size in the present case with an infinite array of holes is significantly reduced, when compared with the case of the plate with a single hole, especially when $R/W = 0.50$. As for the computed normalized T-stress, they are negative in value for all the geometries treated, suggesting low stress triaxiality conditions at the crack-tip. The differences in the trends and magnitudes for the case considered here and that of the finite plate
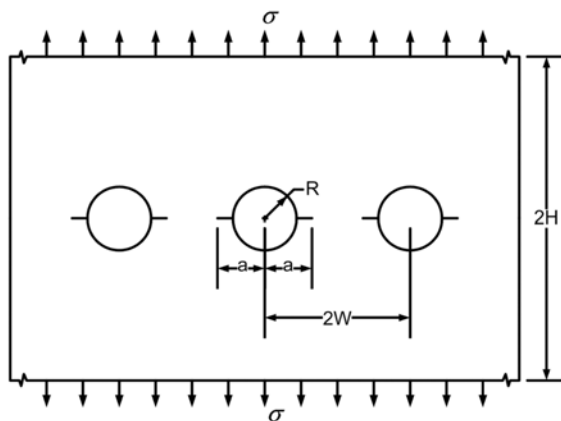

Fig. 4 Case A – A plate with an infinite array of circular holes and with two symmetric cracks emanating from each of them
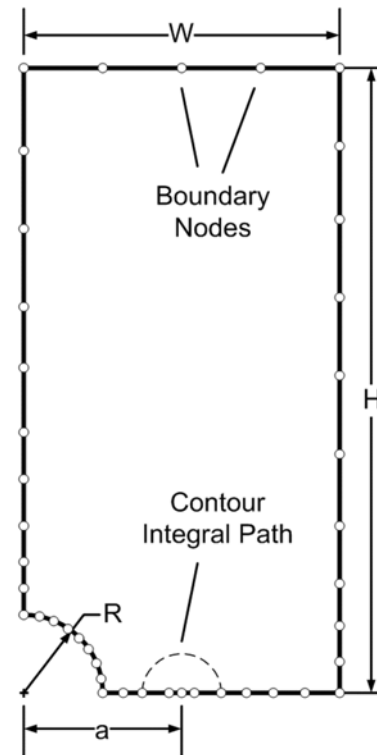
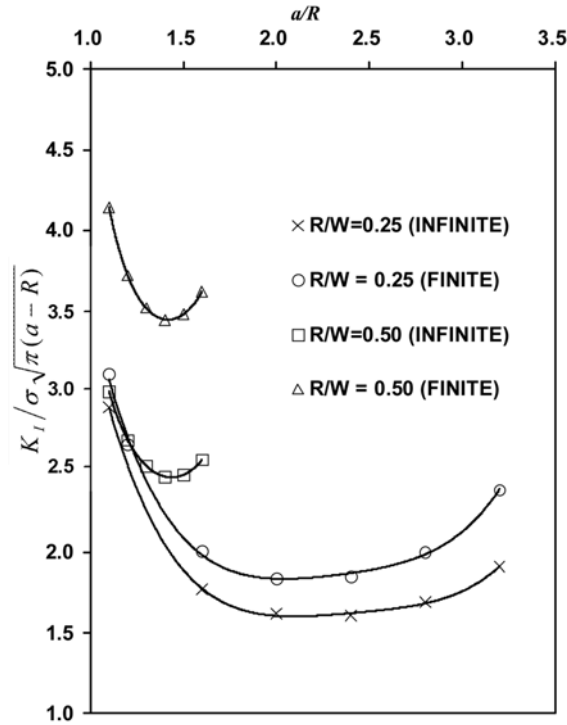Fig. 5 A typical BEM mesh for Case A; $a/R = 2$, $R/W = 0.25$, $H/W = 2$

Fig. 6 Variations of the normalized stress intensity factor, $K_I/\sigma\sqrt{\pi(a-R)}$, with relative crack length – Case A
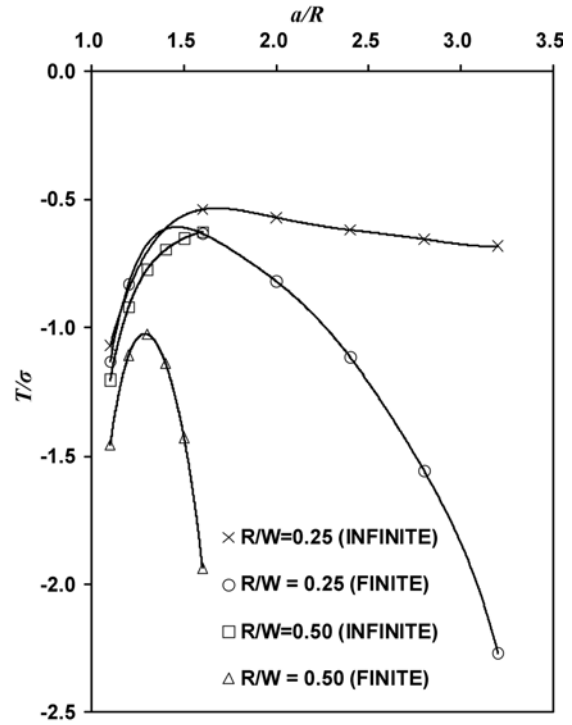
Fig. 7 Variations of the normalized T-stress with relative crack length – Case A

with a single hole are clearly evident. Of interest to note is that when a/R is small, the crack-tip stress constraint increases with increasing crack length up to a certain size of the crack for each set of geometric parameters, as suggested by the decreasing magnitude of the negative T-stress values. With further increase in the crack size, however, the loss of crack-tip stress constraint is relatively small (if at all); this in stark contrast to the finite plate case.

3.2 Case B – A plate with an infinite array of circular holes, each with a crack at its edge

Case B is similar to Case A, except that only one crack emanates from each of the holes, as shown in Fig. 8. The relative crack lengths investigated are the same as those from Case A, for both radii ratios, $R/W = 0.25$ and $R/W = 0.50$. A typical BEM mesh of the model is shown in Fig. 9.

The normalized SIF and T-stress solutions are shown in Figs. 10 and 11, respectively, where they are compared to those of the problem of a finite plate with a hole, Yu *et al.* (2006). It is evident that the trends are similar to those seen in Case A above, and the T-stress values are again negative. For a given relative crack size, the deviations of the magnitudes for the normalized stress intensity factors between Case A and Case B are immediately apparent; however, the same is not true for the T-stress results. This is illustrated in Figs. 12 and 13, where the results of Case A and Case B are compared. For both R/W ratios considered, the T-stress solutions begin to diverge only when $a/R > 1.2$, suggesting that for small relative crack lengths, the T-stress for one crack configuration is also accurate for the other.
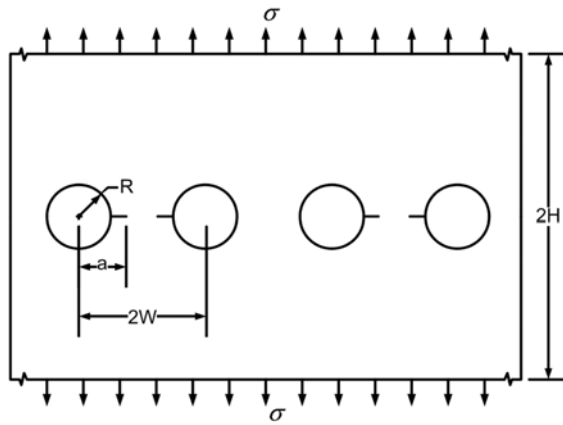
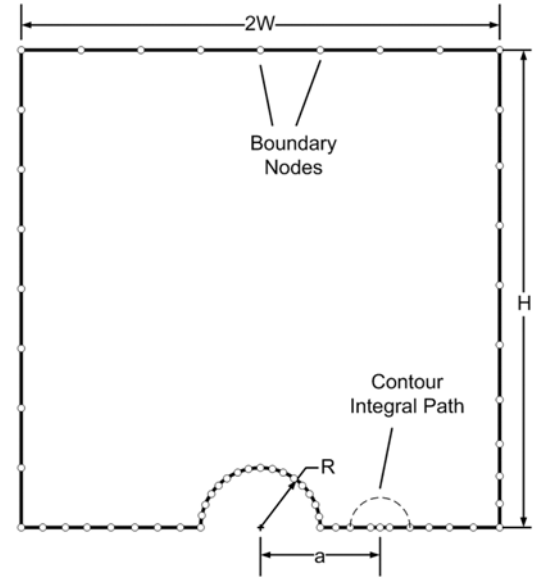Fig. 8 Case B - A plate with an infinite array of circular holes and with a crack emanating from each of them

Fig. 9 A typical BEM mesh for Case B; $a/R = 2$, $R/W = 0.25$, $H/W = 2$
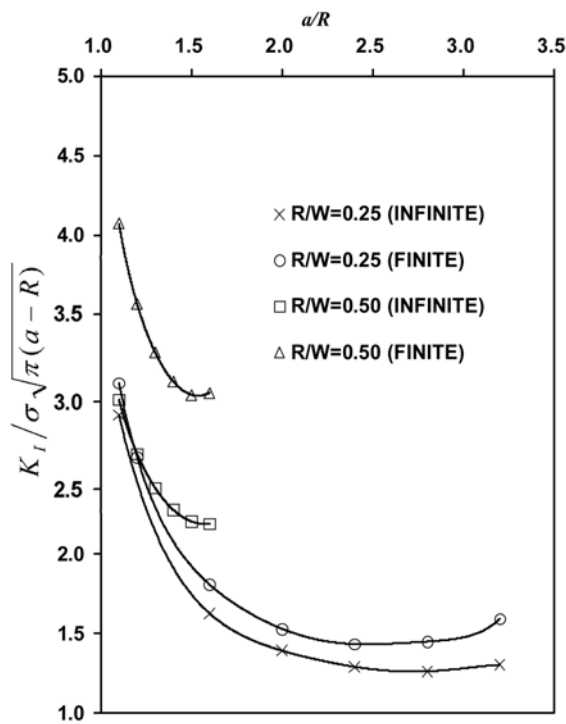

Fig. 10 Variations of normalized stress intensity factors, $K_I/\sigma\sqrt{\pi(a-R)}$, with relative crack length – Case B
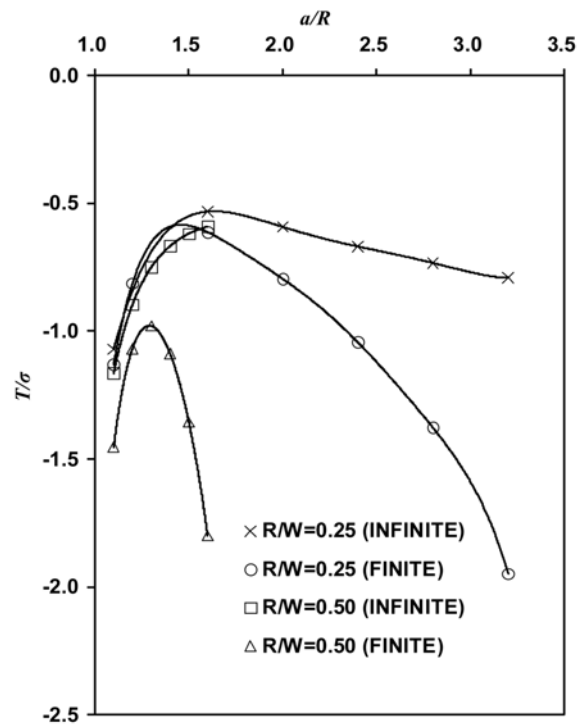

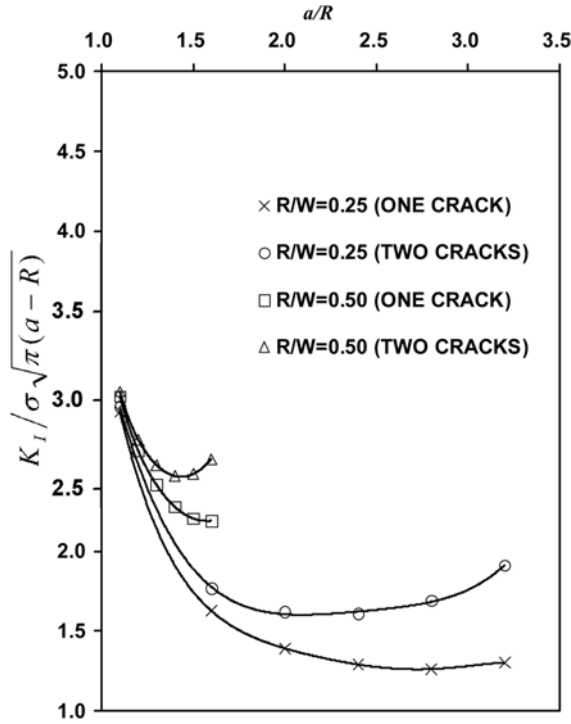Fig. 11 Variations of the normalized *T*-stress with relative crack length – Case B

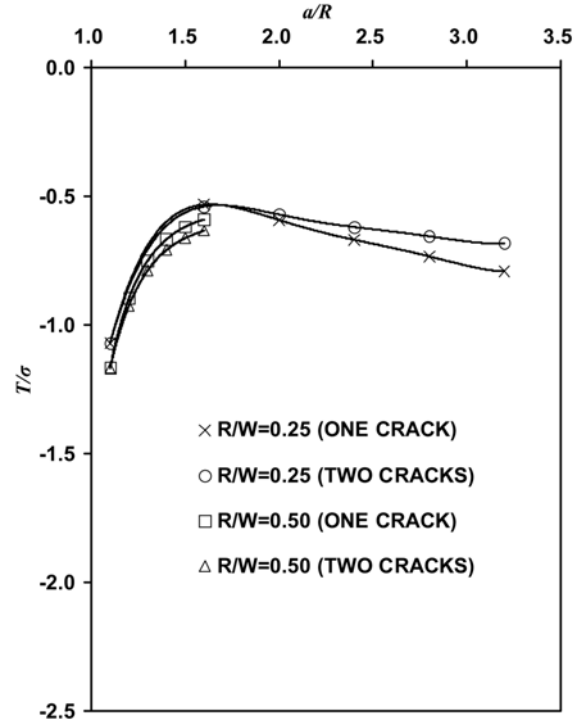Fig. 12 Comparison of SIF solutions, $K_I/\sigma\sqrt{\pi(a-R)}$, between Case A and Case B

Fig. 13 Comparison of T-stress solutions between Case A and Case B

3.3 Case C − An infinite plate with two symmetric cracks emanating from a circular hole in the presence of two other adjacent holes

Fig. 14 shows the physical problem for Case C considered here, where R_1 and R_2 are the radii of the central and the two adjacent holes, respectively, and d is the distance between the holes. Relative crack lengths a/R_1 of $1.1 − 10.0$ were analyzed for relative hole-distance $d* = d/R_1$ of 2.5, 4, 5, 10 and radius ratio $\alpha = R_2/R_1 = 0.25 − 1.0$. Taking advantage of symmetry of the problem, only a quarter of the physical domain needs to be modeled. Fig. 15 shows a typical mesh that was used for this problem. The ratios H/a and $W/a \geq 20$ are used to realize the infinite plate in the analyses.

The BEM results for the normalized SIF, $K_I/\sigma\sqrt{\pi(a-R_1)}$, and the T-stress, T/σ, are listed in Tables 1-4. The qualitative trends of these normalized quantities with increasing crack length are similar to those seen in Case A and Case B as presented in Figs. 12 and 13 above. As noted earlier, for the situation when there are no adjacent holes, $\alpha = 0$, (when $R_2 = 0$), the solutions for both the normalized SIF and T-stress have been presented by Broberg (2004) for all $d*$ ratios treated here. It is perhaps worth mentioning that when $\alpha = 0.25$, the deviations of the normalized stress intensity factors and the T-stress from those given by Broberg (2004) when $\alpha = 0$, are very small indeed (generally less than 2%) for the range of crack sizes and relative hole-distance considered. This is especially true for $a/R_1 < 3$, as the numerical values of both T-stress and K_I are, for all practical purposes, identical.
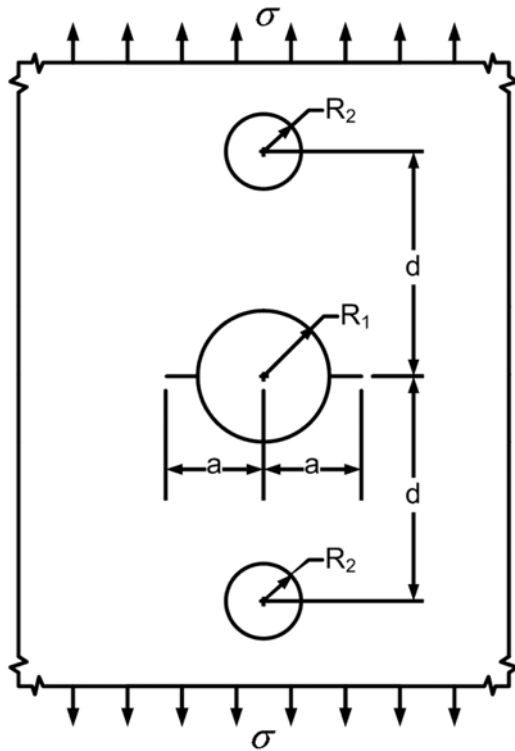
Fig. 14 Case C – A plate with twp symmetric cracks emanating from a circular hole under the influence of adjacent holes

Fig. 15 A typical BEM mesh for Case C; $a/R_1 = 3$, $d/R_1 = 4$, $R_2/R_1 = 0.5$

Table 1 Normalized stress intensity factors, $K_I/\sigma\sqrt{\pi(a-R_1)}$, and normalized *T*-stress, T/σ, for Case C: $\alpha = R_2/R_1$; $d^* = d/R_1 = 2.5$

a/R_1	$K_I/\sigma\sqrt{\pi(a-R_1)}$				T/σ			
	$\alpha = 0.25$	$\alpha = 0.50$	$\alpha = 0.75$	$\alpha = 1.0$	$\alpha = 0.25$	$\alpha = 0.50$	$\alpha = 0.75$	$\alpha = 1.0$
1.1	2.8362	2.7081	2.4700	2.0694	−1.0512	−1.0051	−0.9204	−0.7788
1.2	2.4229	2.3168	2.1258	1.8258	−0.7635	−0.7389	−0.6945	−0.6204
1.4	1.9840	1.9160	1.7882	1.5749	−0.5678	−0.5759	−0.5866	−0.5878
1.6	1.7352	1.6811	1.5963	1.4634	−0.5369	−0.5562	−0.5851	−0.6177
2.0	1.4892	1.4718	1.4249	1.3605	−0.6018	−0.6251	−0.6621	−0.7066
3.0	1.2955	1.2941	1.2905	1.2844	−0.7859	−0.7942	−0.8078	−0.8241
4.0	1.2357	1.2372	1.2400	1.2453	−0.8905	−0.8902	−0.8890	−0.8835
10.0	1.1129	1.1137	1.1157	1.1181	−1.0067	−1.0010	−0.9904	−0.9722

Table 2 Normalized stress intensity factors, $K_I/\sigma\sqrt{\pi(a-R_1)}$, and normalized T-stress, T/σ, for Case C: $\alpha = R_2/R_1$; $d^* = d/R_1 = 4.0$

a/R_1	$K_I/\sigma\sqrt{\pi(a-R_1)}$				T/σ			
	$\alpha = 0.25$	$\alpha = 0.50$	$\alpha = 0.75$	$\alpha = 1.0$	$\alpha = 0.25$	$\alpha = 0.50$	$\alpha = 0.75$	$\alpha = 1.0$
1.1	2.8396	2.7324	2.5552	2.3149	−1.0541	−1.0159	−0.9509	−0.8636
1.2	2.4280	2.3430	2.2026	2.0125	−0.7649	−0.7421	−0.7043	−0.6526
1.4	1.9828	1.9188	1.8122	1.6655	−0.5647	−0.5605	−0.5528	−0.5391
1.6	1.7505	1.7023	1.6227	1.5118	−0.5383	−0.5415	−0.5455	−0.5486
2.0	1.5055	1.4760	1.4267	1.3568	−0.6109	−0.6223	−0.6393	−0.6595
3.0	1.2924	1.2838	1.2679	1.2443	−0.7881	−0.8001	−0.8188	−0.8422
4.0	1.2340	1.2316	1.2262	1.2186	−0.8935	−0.9007	−0.9126	−0.9287
10.0	1.1126	1.1129	1.1137	1.1147	−1.0214	−1.0076	−1.0049	−1.0022

Table 3 Normalized stress intensity factors, $K_I/\sigma\sqrt{\pi(a-R_1)}$, and normalized T-stress, T/σ, for Case C: $\alpha = R_2/R_1$; $d^* = d/R_1 = 5.0$

a/R_1	$K_I/\sigma\sqrt{\pi(a-R_1)}$				T/σ			
	$\alpha = 0.25$	$\alpha = 0.50$	$\alpha = 0.75$	$\alpha = 1.0$	$\alpha = 0.25$	$\alpha = 0.50$	$\alpha = 0.75$	$\alpha = 1.0$
1.1	2.8458	2.7640	2.6291	2.4452	−1.0575	−1.0274	−0.9782	−0.9109
1.2	2.4323	2.3687	2.2642	2.1200	−0.7667	−0.7488	−0.7191	−0.6784
1.4	1.9859	1.9346	1.8503	1.7343	−0.5647	−0.5581	−0.5468	−0.5304
1.6	1.7528	1.7142	1.6501	1.5611	−0.5375	−0.5355	−0.5320	−0.5263
2.0	1.5059	1.4797	1.4361	1.3750	−0.6096	−0.6132	−0.6187	−0.6251
3.0	1.2922	1.2810	1.2624	1.2365	−0.7879	−0.7960	−0.8086	−0.8249
4.0	1.2331	1.2288	1.2213	1.2106	−0.8944	−0.9015	−0.9131	−0.9284
10.0	1.1118	1.1134	1.1142	1.1142	−1.0079	−1.0080	−1.0087	−1.0086

Table 4 Normalized stress intensity factors, $K_I/\sigma\sqrt{\pi(a-R_1)}$, and normalized T-stress, T/σ, for Case C: $\alpha = R_2/R_1$; $d^* = d/R_1 = 10.0$

a/R_1	$K_I/\sigma\sqrt{\pi(a-R_1)}$				T/σ			
	$\alpha = 0.25$	$\alpha = 0.50$	$\alpha = 0.75$	$\alpha = 1.0$	$\alpha = 0.25$	$\alpha = 0.50$	$\alpha = 0.75$	$\alpha = 1.0$
1.1	2.8508	2.8229	2.7655	2.7104	−1.0577	−1.0479	−1.0421	−1.0117
1.2	2.4352	2.4147	2.3690	2.3284	−0.7655	−0.7597	−0.7582	−0.7379
1.4	1.9827	1.9644	1.9285	1.8898	−0.5615	−0.5572	−0.5561	−0.5422
1.6	1.7466	1.7325	1.7025	1.6747	−0.5307	−0.5274	−0.5289	−0.5171
2.0	1.4918	1.4807	1.4572	1.4324	−0.5959	−0.5928	−0.5963	−0.5796
3.0	1.2686	1.2611	1.2464	1.2308	−0.7700	−0.7678	−0.7735	−0.7628
4.0	1.1942	1.1889	1.1791	1.1677	−0.8672	−0.8665	−0.8727	−0.8667
10.0	1.0805	1.0801	1.0809	1.0790	−0.9822	−0.9834	−0.9867	−0.9882

It is also evident from the results shown in the tables that as the hole radii ratio α increases, its effects on the stress intensity factor as well as the T-stress are most pronounced when the hole-distance ratio d^* is the smallest, particularly for shorter cracks. For example, when $d^* = 2.5$ and

relative crack length $a/R_1 = 1.1$, a reduction by 37% and 35% in the magnitudes of the normalized SIF and the *T*-stress, respectively, are noted when the hole radius ratio α is increased from 0.25 to 1.0. As $d*$ is increased to 10.0, the corresponding decreases of the magnitudes of these normalized fracture parameters for the same crack size are only about 5%. As the crack gets progressively longer, as expected, the influence of the adjacent holes becomes also less significant; indeed, when $a/R_1 > 4$, the effects of the adjacent holes are minimal for all the geometries analyzed in this Case C.

It is important to note that in all the three cases analyzed here, the *T*-stress decreases as the crack becomes smaller and smaller. It is expected since the stress field is controlled by the stress concentration when the crack is small. As discussed by Wang *et al.* (2006), the normalized *T*-stress at the limit $(a - R)/R \to 0$ equals $-0.526 K_t$ (K_t is the stress concentration factor of the hole). As the crack size increases, the effect of the local stress concentration becomes less and the *T*-stress solutions converge to the long crack solutions.

4. Conclusions

The Boundary Element Method has been employed to determine *T*-stress solutions for cracks emanating from circular holes in infinitely wide plates under remote uniform tension. This fracture parameter is increasing being recognized as an important additional quantity to the stress intensity factor in order to provide better failure assessments of cracked components. In this study, three geometric cases of the cracked plate with multiple circular holes have been considered. For the sake of completeness, stress intensity factor solutions have also been obtained for these geometries. Numerical values of the *T*-stress obtained are all negative for all the cases treated, signifying low stress triaxiality conditions at the crack-tips. However, their magnitudes are smaller than the corresponding ones for cracks of the same size in plates of finite width with just a circular hole which have the same effective net un-cracked ligament. One of the problems investigated involved the presence of two adjacent holes to the one from which cracks have emanated; the centres of these holes lie in a plane perpendicular to the cracks. It is found in this case, these adjacent holes only have significant influence on the *T*-stress when the crack sizes are relatively small.

Acknowledgements

References

Ainsworth, R.A., Bannister, A.C. and Zerbst, U. (2002), "An overview of the european flaw assessment procedure sintap and its validation", *Int. J. Pressure Vessel & Piping*, **77**, 869-876.
Ainsworth, R.A., Sattari-Far, I., Sherry, A.H., Hooten, D.G. and Hadley, I. (2000), "Methods of including constraint effects within SINTAP procedures", *Eng. Fract. Mech.*, **67**, 563-571.
Aliabadi, M.H. and Rooke, D.P. (1986), *Numerical Fracture Mechanics*. Kluwer Academic Publishers, Dordrecht.

Betegon, C. and Hancock, J.W. (1991), "Two-parameter characterization of elastic-plastic crack tip field", *J. Appl. Mech.*, ASME, **58**, 104-110.

Bilby, B.A., Cardew, G.E., Goldthorpe, M.R. and Howard, I.C. (1986), "A finite element investigation of the effect of specimen geometry on the fields of stress and strains at the tips of stationary cracks", In: *Size Effects in Fracture*, Mechanical Engineering Publications, London, 37-46.

Broberg, K.B. (2004), "A note on *T*-stress determination using dislocation arrays", *Int. J. Fracture*, **131**, 1-14.

Du, Z.Z. and Hancock, J.W. (1991), "The effect of non-singular stresses on crack tip constraint", *J. Mech. Physics Solids*, **39**, 555-567.

Kfouri, A.P. (1986), "Some evaluations of the elastic *T*-stress using Eshelby's method", *Int. J. Fract.*, **20**, 301-315.

Larsson, S.G. and Carlsson, A.J. (1973), "Influence of non-singular stress terms and specimen geometry on small-scale yielding at crack-tips in elastic-plastic materials", *J. Mech. Physics Solids*, **21**, 263-277.

Lewis, T. (2005), "*T*-stress solutions for cracks at notches and in cylinders", M.A.Sc. Thesis, Carleton University, Ottawa, ON, Canada.

Li, J., Tan, C.L. and Wang, X. (2004), "*T*-stress solutions for a radial edge crack in a thick-walled cylinder by the boundary element method", In: Leitao, V.M.A. and Aliabadi, M.H. (eds.) *Advances in Boundary Element Techniques V*, Proceedings of BETEQ 2004 Conference, Lisbon, EC Ltd., U.K., 141-146.

Murakami, Y. (2003), *Stress Intensity Factors Handbook*. Pergamon Press, Elmsford, New York.

Rice, J.R. (1974), "Limitations to small scale yielding approximation for crack tip plasticity", *J. Mech. Physics Solids*, **22**, 17-26.

Rooke, D.P. and Cartwright, D.J. (1976), *Compendium of Stress Intensity Factors*. Hillington Press, Uxbridge, Middx (UK).

Roychowdhury, S. and Dodds, R.H. (2004), "Effects of T-stress on fatigue crack closure in 3-D small scale yielding", *Int. J. Solids Struct.*, **41**, 2581-2606.

Shah, P.D., Tan, C.L. and Wang, X. (2005), "*T*-stress solutions for two-dimensional crack problems in anisotropic elasticity using the boundary element method", *Fatigue Fract. Engng. Mater. Struct.*, **29**, 343-356.

Sladek, J., Sladek, V. and Fedelinski, P. (1997), "Contour integrals for mixed-mode crack analysis: effect of non-singular terms", *Theo. Appl. Fract. Mech.*, **27**, 115-127.

Tong, J. (2002), "*T*-stress and its implications for crack growth", *Eng. Fract. Mech.*, **69**, 1325-1337.

Wang, X., Lewis, T. and Bell, R. (2006), "Estimations of the *T*-stress for small cracks at notches", *Eng. Fract. Mech.*, **73**, 366-375.

Williams, M.L. (1957), "On the stress distribution at the base of a stationary crack", *J. Appl. Mech.*, ASME, **24**, 109-114.

Yu, J., Tan, C.L. and Wang, X. (2006), "*T*-stress solutions for cracks emanating from a circular hole in a finite plate", *Int. J. Fract.*, **140**, pp. 293-298.